Supporting Information

Fluorinated Polymer Electrolyte via Dual-Salt Coupling for Solid-State Lithium Metal Batteries

Yayue He,[a] Shuangshuang Zhu,[b] Shilun Gao,*[,c] Xuan Liu,[a] Zhenxi Li,[b] Yurong Liang,[a] Yan Zhai,[a] Pengfei Cao,[d] and Huabin Yang*[,b,e]

[a] Department of Materials Engineering, Taiyuan Institute of Technology, Shanxi, Taiyuan 030008, China.

[b] Institute of New Energy Material Chemistry, School of Materials Science and Engineering, Nankai University, Tianjin 300350, China.

[c] School of Integrated Circuit Science and Engineering, Tianjin University of Technology, Tianjin 300384, China.

[d] State Key Laboratory of Organic-Inorganic Composites, Beijing University of Chemical Technology, Beijing 100029, China.

[e] Tianjin Key Laboratory of Metal and Molecular Based Material Chemistry, School of Materials Science and Engineering, Nankai University, Tianjin 300350, China.

[†] E-mail addresses: gaoshilun@nankai.edu.cn (Shilun Gao), hb_yang@nankai.edu.cn (Huabin Yang).

Experimental Section

Materials: Polyethylene glycol (PEG, M_n = 600 g mol^{-1}), 2-isocyanatoethyl acrylate (ICEA), 2,2,3,4,4,4-hexafluorobutyl acrylate (HFBA), succinonitrile (SN), butyl acrylate (BA), 2,2'-Azobis(2-methylpropionitrile) (AIBN), Tetrahydrofuran (THF), lithium bis(trifluoromethanesulfonimide) (LiTFSI), and lithium bis(lithium dicarbonate borate) (LiBOB) were purchased from Aladdin. All materials were used as purchased, without further purification.

Preparation of A-PEG: The terminal unsaturation of acrylate-functionalized polyethylene glycol (A-PEG) was obtained by the reaction of polyethylene glycol (PEG, Aladdin) and 2-isocyanatoethyl acrylate (ICEA, Aladdin) with molar ratio of 2/3, dissolving in THF (J&K Scientific, Extra Dry). The reaction was performed with a 5 mol% catalyst (dibutyltin dilaurate, DBTDL, Aladdin) for 6 h under 80 °C magnetic stirring under argon (Ar) protection. The solvent was removed by rotary evaporator and PEG was dehydrated before use.

Preparation of precursor solution: Firstly, lithium salts (LiTFSI or a mass ratio of 8/2 mixture of LiTFSI and LiBOB) with a concentration of 2 M were fully dissolved in SN to obtain the SN solution. Secondly, the prepared A-PEG was mixed with HFBA in a molar ratio of 1/1, and 0.5 mol% of AIBN initiator was added. The mixture was stirred thoroughly to obtain the monomer mixture solution. The SN solution was then mixed with the above monomer mixture solution in a mass ratio of 1/1, stirred fully at room temperature to dissolve, and the precursor solution for the solid electrolyte was prepared. All the above processes were carried out in a glove box filled with argon, with both O_2 and H_2O levels maintained below 0.1 ppm.

Preparation of D-PFPS: The precursor solution was polymerized in-situ by thermal initiation at 70 °C for 6 h to prepare the in-situ solid electrolyte. Celgard 2400 separator was used to assemble a CR2032 coin cell. The precursor solution was dropped on both sides of the separator with 50 μL, and after thorough impregnation, the assembled cell was polymerized at 70 °C for 6 h to obtain a solid-state battery.

Material characterization: Fourier transform infrared (FT-IR) spectra were recorded on a Nicolet iS50 FT-IR spectrometer (Bruker Tensor II) in the scanning range of 4000−400 cm^{-1}. Thermogravimetric analysis (TGA) was carried out using a TG-DTA8122 instrument at a scanning rate of 10 °C/min under an N_2 atmosphere. The morphology of the electrodes was observed by a scanning electron microscope (SEM, JSM-7800F, JEOL, Japan). The Raman spectra was collected using a TEO Raman microscope (SR-500I-A) with 532 nm laser. X-ray photoelectron spectroscopy (XPS) spectra were recorded from the Thermo Scientific ESCALAB 250Xi system. Before SEM and XPS characterizations, the samples were rinsed with pure DME or DMC solvent to remove the residual lithium salts and electrolyte and dried under a vacuum in the glovebox mentioned above. Then they were transferred into these instruments with a special sealed device to avoid air exposure.

Battery assembly and measurement: For the cathode, $LiFePO_4$(LFP, HF-Kejing), Super P, and poly(vinylidene fluoride) binder (Kynar HSV900, ARKEMA) with the weight of 8:1:1 and then mixed with N-methylpyrrolidionon as the solvent. The slurry was first coated on an Al foil, which was then placed in a vacuum oven at 120 °C for 12 h. The mass loading of the LFP cathode was ~2 mg cm^{-2} and 8 mg cm^{-2}. The NMC811 (HF-Kejing) cathodes with a mass loading of 2 mg cm^{-2} were also prepared following the same procedure.

The CR 2032-type coin cells were assembled in an Ar-filled glovebox with O_2 and H_2O contents below 1.0 ppm.

The Li^+ transference number (strictly speaking, cationic transport number t_{Li^+}) was obtained via the potentiostatic polarization method in a symmetric Li/electrolyte film/Li cell according to the following equation:

$$t_{Li+} = I_s(\Delta V - I_0R_0)/I_0(\Delta V - I_sR_s)$$

where I_0 and R_0 are the initial current and resistance, respectively, and I_s and R_s are the steady-state current and resistance after the polarization, respectively.

The ionic conductivity was obtained from the impedance measurements via the following equivalence

$\sigma = l/RS$

where l and S are the electrolyte film thickness (cm) and contact area (cm^2), respectively, and R is the ohmic resistance (Ω). R of electrolytes films was determined at room temperature by assembling electrolytes discs (Φ, ~16 mm) in 2032-type coin cells sandwiched between two steel spacers and using electrochemical impedance spectroscopy (EIS) on a Zennium Pro Electrochemical System in the frequency range of 1 MHz to 10 mHz with an amplitude of 5 mV.

Density functional theory (DFT): The lowest unoccupied molecular orbital (LUMO) energy levels calculations were carried out by using the Gaussian 09 W program, and the molecular geometries for the ground states were optimized at the B3LYP/6-311G(d,p) level.

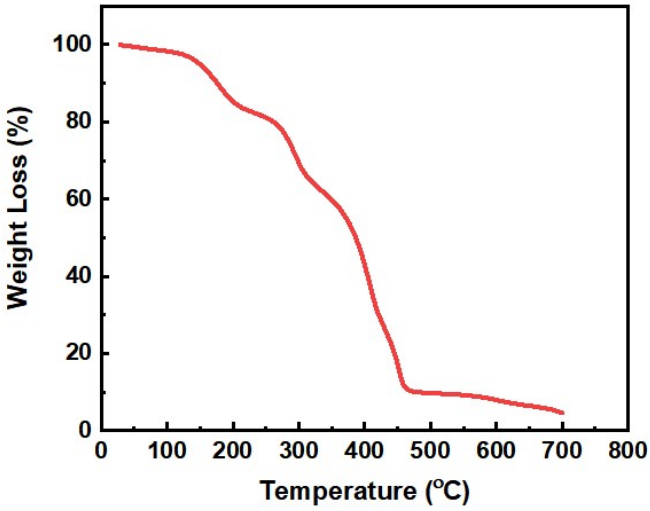

Fig. S1 TG curve of fluorinated polymer electrolytes.

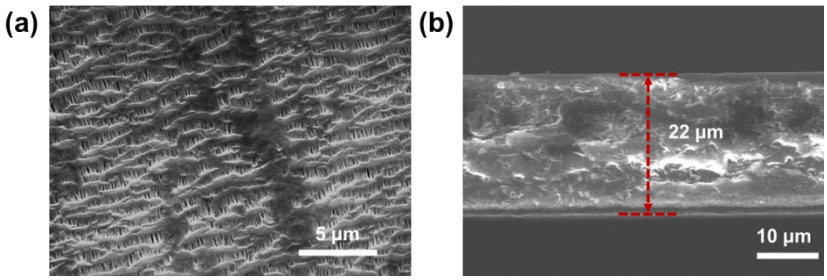

Fig. S2 Surface morphologies (a) and cross-sectional morphologies (b) of PP separator.

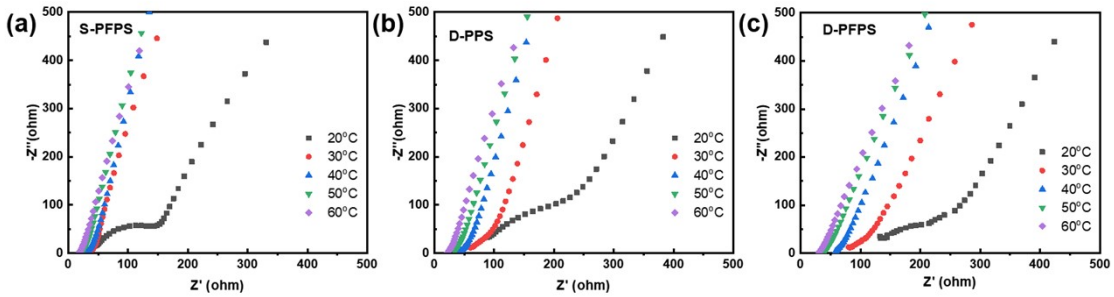

Fig. S3 Nyquist curves of S-PFPS (a), D-PPS (b) and D-PFPS (c) ranging from 20 to 60 °C.

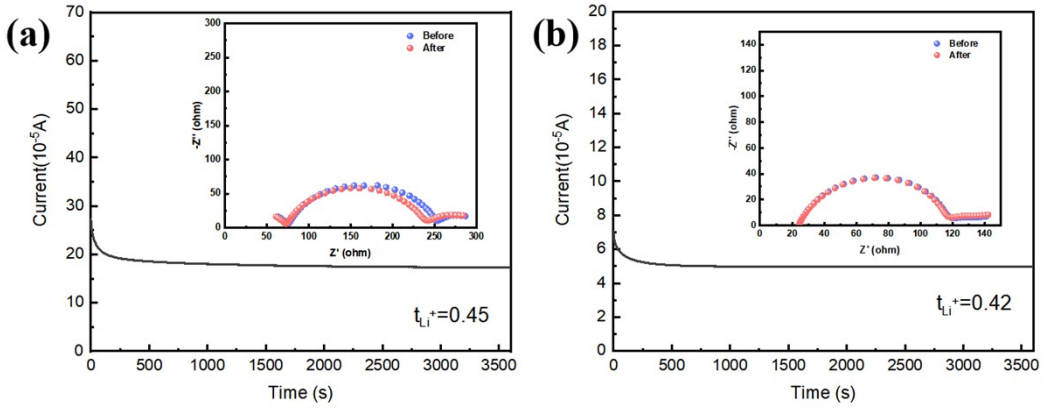

Fig. S4 The chronoamperometry profile of a symmetric Li/S-PFPS/Li cell (a) and Li/D-PPS/Li cell (b) under a polarization voltage of 10 mV, and the EISs before and after the polarization (inset).

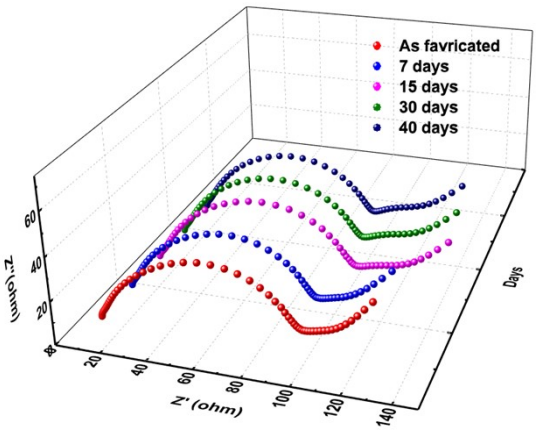

Fig. S5 Electrochemical impedance spectra of the Li/D-PFPS/Li batteries stored under open-circuit condition at 60 °C.

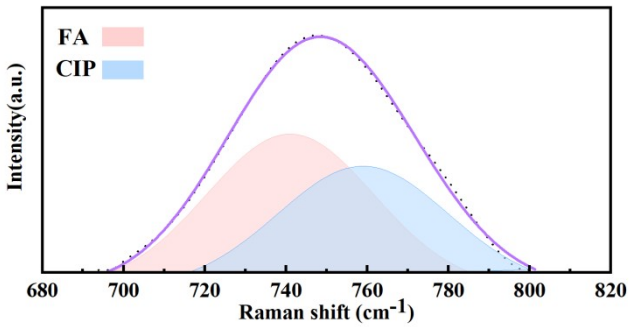

Fig. S6 Raman spectrum of the D-PFPS.

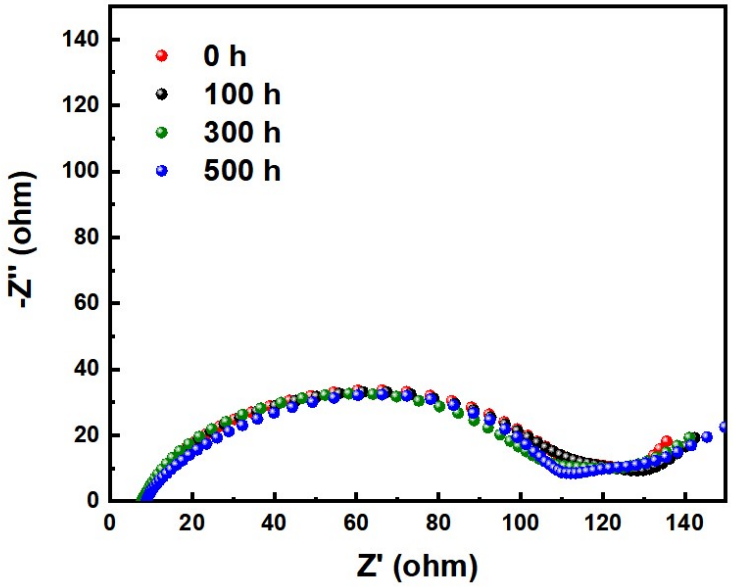

Fig. S7 Electrochemical impedance spectra of the Li/D-PFPS/Li batteries during the cycling process at 60 °C.

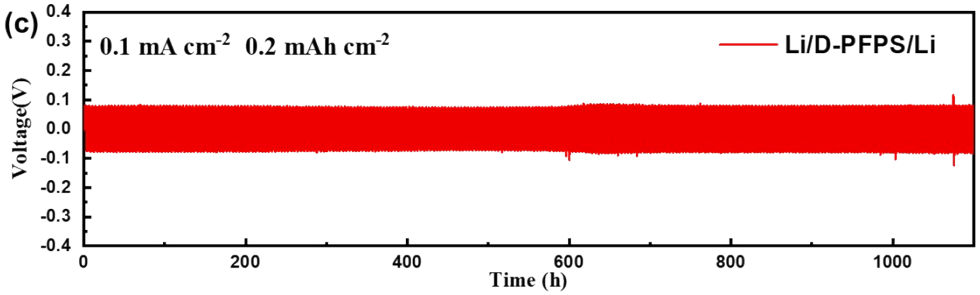

Fig. S8 The long cycling performance of Li/D-PFPS/Li symmetrical cell at 0.1mA cm^{-2} and 0.2 mAh cm^{-2}.

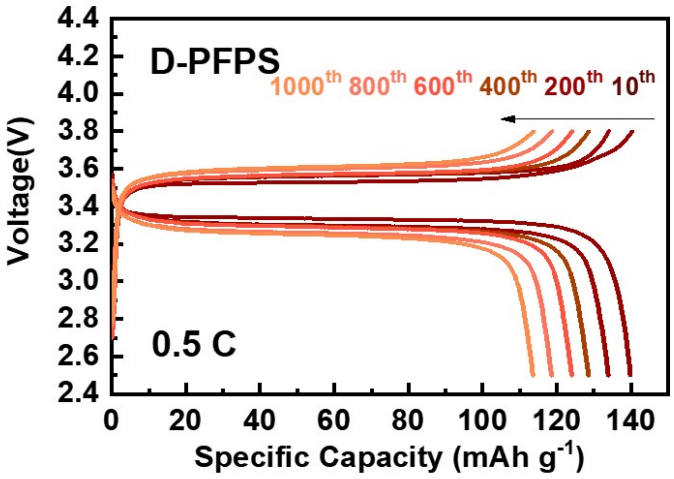

Fig. S9 Capacity voltage curves of LFP/D-PFPS/Li full cell at 60 °C and 0.5C with different number of cycles.

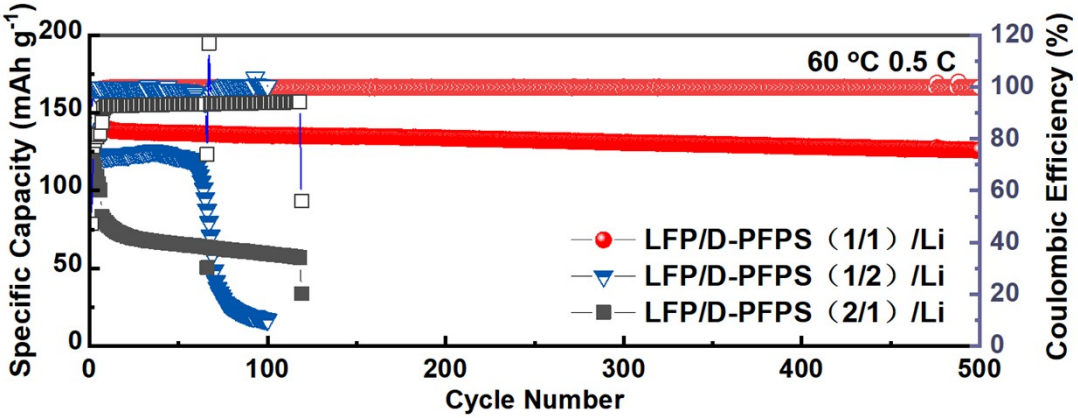

Fig. S10 Electrochemical performance of LFP/D-PFPS/Li full cells with polymer-to-plastic crystal mass ratios of 1/1, 2/1, and 1/2 at 0.5 C and 60 °C.

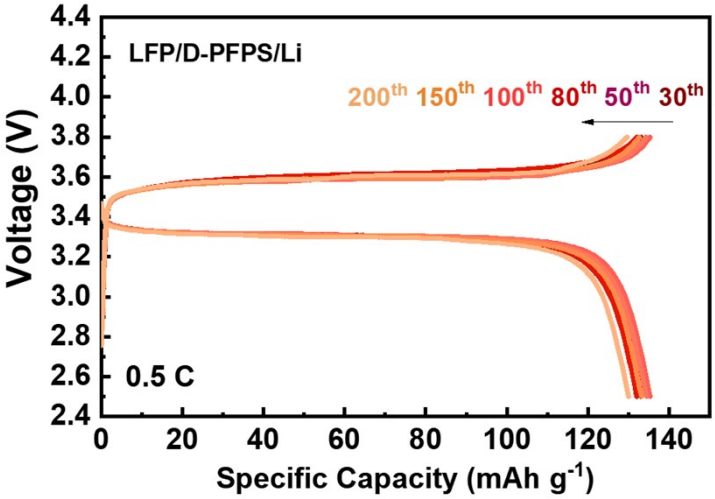

Fig. S11 Capacity voltage curve of LFP/D-PFPS/Li full cell at 25 ºC and 0.5C with different number of cycles.

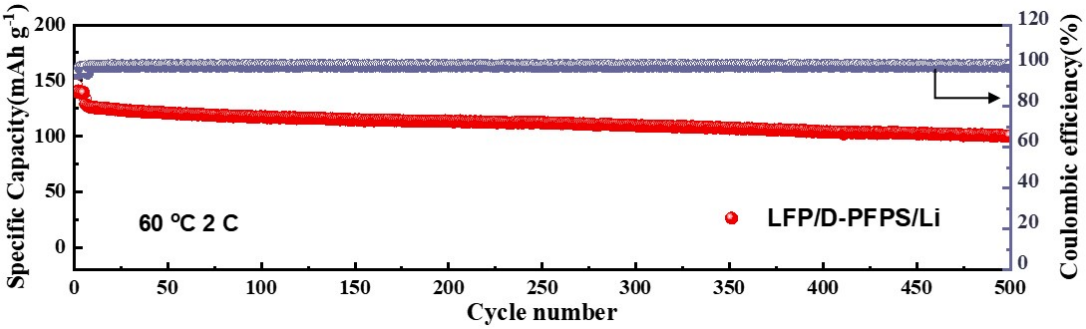

Fig. S12 Electrochemical performance of LFP/D-PFPS/Li full cell at 2C and 60 °C.

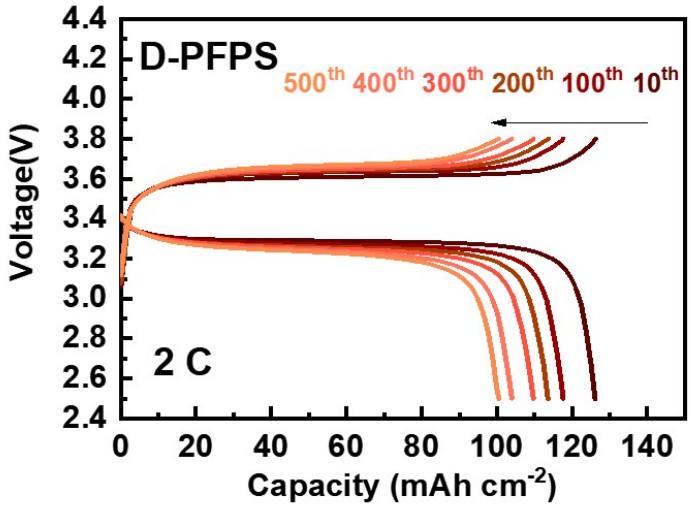

Fig. S13 Capacity voltage curve of LFP/D-PFPS/Li full cell with different number of cycles.

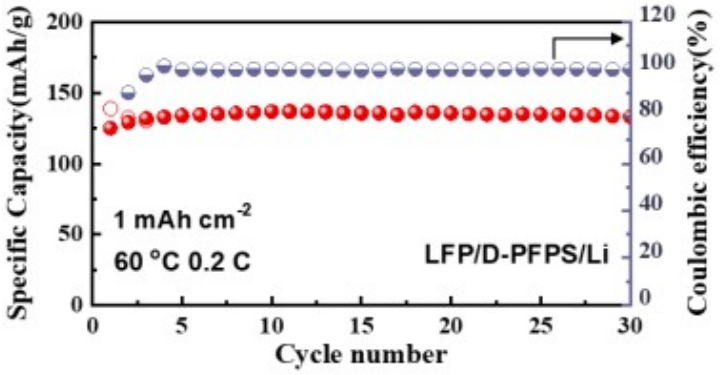

Fig. S14 Electrochemical performance of LFP/D-PFPS/Li full cell at 0.2C and 60 °C with the cathode mass loading of 7 mg cm^{-2}.

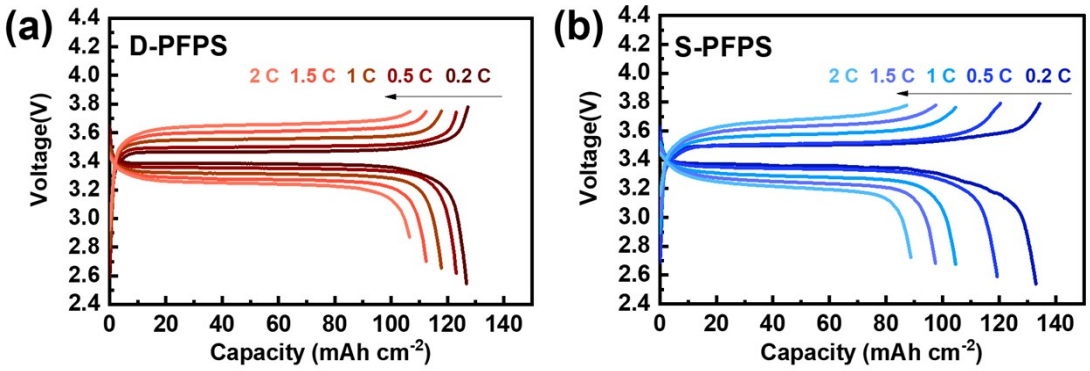

Fig. S15 (a) Capacity voltage curve of LFP/D-PFPS/Li full cell with different number of cycles. (b) Capacity voltage curve of LFP/S-PFPS/Li full cell with different number of cycles.

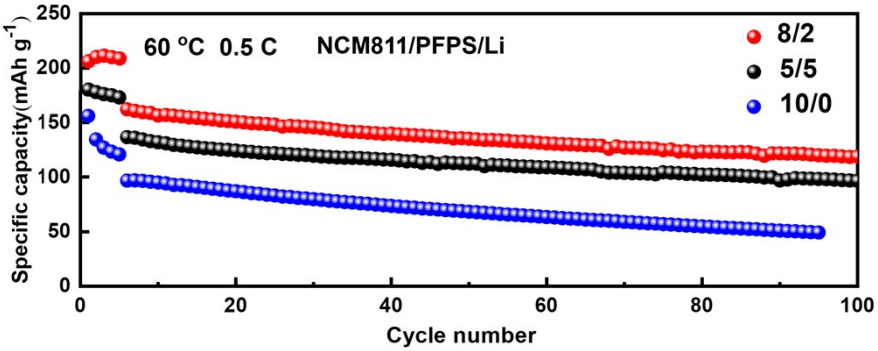

Fig. S16 Electrochemical performance of NCM811/PFPS/Li full cells with LiTFSI-LiBOB salt ratios of 8/2, 5/5, and 10/1 at 0.5C and 60 °C.